Molecular Crystals and Liquid Crystals Science and Technology. Section A. Molecular Crystals and Liquid Crystals

Publication details, including instructions for authors and subscription information:
http://www.tandfonline.com/loi/gmcl19

Smectic C Twist Grain Boundary Phase (TGB_C) Under External Electric Field

P. Barois [a] , M. Nobili [a] & M. Petit [a]

[a] Centre de Recherche Paul-Pascal, Avenue A. Schweitzer, F-33600, Pessac, FRANCE

Version of record first published: 04 Oct 2006

To cite this article: P. Barois, M. Nobili & M. Petit (1997): Smectic C Twist Grain Boundary Phase (TGB_C) Under External Electric Field, Molecular Crystals and Liquid Crystals Science and Technology. Section A. Molecular Crystals and Liquid Crystals, 302:1, 215-221

To link to this article: http://dx.doi.org/10.1080/10587259708041831

Mol. Cryst. Liq. Cryst., 1997, Vol. 302, pp. 215–221
Reprints available directly from the publisher
Photocopying permitted by license only

SMECTIC C TWIST GRAIN BOUNDARY PHASE (TGB_C) UNDER EXTERNAL ELECTRIC FIELD

P. BAROIS, M. NOBILI and M. PETIT
Centre de Recherche Paul-Pascal, Avenue A. Schweitzer, F-33600 Pessac, FRANCE

Abstract We modelize the behavior of a TGB_C under an external electric field applied perpendicular to the pitch direction. A comparaison with x-ray diffraction measurements is presented.

INTRODUCTION

Pointed out by de Gennes in 1972[1], the analogy between the nematic (N) to smectic-A (SmA) transition in liquid crystals and the normal to superconductor transition in metals[2] has been beautifully illustrated by the discovery of a helical smectic-A phase in chiral liquid crystals[3]. The highly dislocated structure of this new phase called twist grain boundary phase (TGB_A) has been proposed in 1988 by Renn and Lubensky (RL)[4]: slabs of smectic-A material (i.e. superconducting phase in the analogy) of thickness ℓ_b are regularly stacked in a helical fashion along an axis parallel to the smectic layers. Adjacent slabs are continuously connected via a grain boundary constituted of a grid of parallel equispaced screw dislocation lines analogous to magnetic vortices. The nematic director $\mathbf{n}$, and hence the smectic layer normal $\mathbf{N}$, is rotated across each grain boundary by an angle $\Delta\Theta$ given by:

$$\Delta\Theta = 2\arcsin(d/(2\ell_d)) \approx d/\ell_d, \tag{1}$$

where d is the smectic period and ℓ_d the distance between parallel dislocation lines.

In agreement with RL expectations, a second TGB phase was identified namely TGB_C in which the smectic slabs are SmC i.e. $\mathbf{n} \cdot \mathbf{N} = \cos\theta \neq 1$[5,6]. The TGB_C phase however turns out to be more complex than first expected. First of all, commensurate x-ray diffraction patterns are commonly observed on well aligned TGB_C samples, i.e. the grain boundary angle $\Delta\Theta$ is a rational fraction of 2π[6,7]. The origin of this commensurability is so far unexplained[8]. Moreover, the TGB_C structure has a priori one more degree of freedom than TGB_A, namely, the orientation of the vector $\mathbf{n} \times \mathbf{N}$ parallel to the spontaneous electric polarization $\mathbf{P}_s$ of each slab[9]. RL described the TGB_C structure with the assumption that the smectic layer normal $\mathbf{N}$ remains perpendicular to the pitch direction[10,11] $\hat{\mathbf{x}}$ just like in the TGB_A phase. This in turn implies that the director $\mathbf{n}$ is also perpendicular to $\hat{\mathbf{x}}$ and the spontaneous electric polarization $\mathbf{P}_s$ of each smectic slab lies along

$\hat{\mathbf{x}}$: the RL TGB_C structure is thus ferroelectric. X-ray diffraction experiments on well aligned TGB_C sample showed that this assumption is not valid: the layer normal $\mathbf{N}$ is tilted instead by an angle ω_L relative to the plane (y,z) perpendicular to the pitch direction $\hat{\mathbf{x}}$[12]. It is suggested in reference 12 that the director field $\mathbf{n}$ of the TGB_C phase still lies in the (y,z) plane like in the cholesteric phase. This assumption which minimizes the bend term $(1/2)K_{33}(\mathbf{n}\times\nabla\times\mathbf{n})^2$ of the Frank energy is possible since the angle ω_L equals the SmC tilt angle within experimental accuracy. It implies that the spontaneous electric polarization $\mathbf{P}_s$ of each SmC slab is orthogonal to the pitch axis and precedes in a helical fashion about it. We call this helical arrangement of local polarizations helielectric. The space distribution of the local polarizations can in principle be tested through electric properties of the phase.

In this paper, we report a first model of the TGB_C behavior under an external electric field. A transverse electric field (i.e. perpendicular to the TGB_C helical axis) couples with the spontaneous polarization of each TGB_C block; as a result, the thickness of blocks with polarization parallel to the field increases. At the same time, the thickness of block with polarization anti-parallel to the field decreases. In low electric field, the polarization reoriention along the field direction can be considered negligible as we will show. A comparison with experimental results will be presented.

TGB_C UNDER A TRANSVERSE ELECTRIC FIELD

Let us consider a TGB_C slab sandwiched between two parallel surfaces. The TGB_C helical axis $\hat{\mathbf{x}}$ coincides with the normals to the surfaces. We assume the nematic director $\mathbf{n}$ uniform in each block. $\mathbf{n}$ and the spontaneous polarization $\mathbf{P}_s \parallel (\mathbf{N}\times\mathbf{n})$ of each block precess in helical fashion in the plane (y,z) (see Figure 1). The director is anchored at the surfaces along the axis $\hat{\mathbf{z}}$. The TGB_C is homogeneous in planes parallel to the surfaces. An electric field $\mathbf{E}$ is applied along the $\hat{\mathbf{y}}$-axis. The angle between $\mathbf{n}$ and the normal to the smectic plane $\mathbf{N}$ and, as consequence $|\mathbf{P}_s|$, is assumed to be independent on the electric field amplitude. The i^{th}-block energy per unit surface area f_i in the electric field $\mathbf{E}$ writes as:

$$f_i = -\int_{block} \mathbf{P}_s \cdot \mathbf{E} dx = -P_s E s_i \cos\theta_i, \tag{2}$$

where s_i and θ_i are the thickness and the angle between $\mathbf{n}$ and $\hat{\mathbf{y}}$-axis for the i^{th}-block, respectively. To minimize f_i (2) there are two possibilities; the first one is to increase the thickness s_i of the blocks with polarization parallel to $\mathbf{E}$ ($\theta_i \approx 0$) and to decrease, at the same time, the block thickness which polarization anti-parallel to $\mathbf{E}$ ($\theta_i \approx \pi$). The second one is to keep s_i constant and to reorient the polarization of each block along the electric field. In general both mechanisms act at the same time.

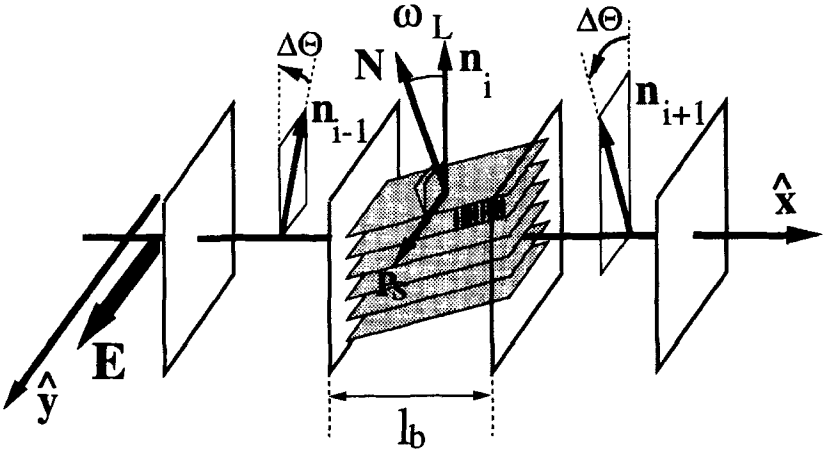

FIGURE 1 TGB$_C$ helielectric model: local spontaneous polarizations $\mathbf{P}_s$ are perpendicular to $\hat{\mathbf{x}}$ at angle θ_i relative to the field direction $\hat{\mathbf{y}}$. In absence of field, the slab thickness s_i and the twist angles $\theta_{i+1} - \theta_i$ are equal to ℓ_b and $\Delta\Theta$, respectively.

TGB FREE ELASTIC ENERGY

Gains in the electric energy (2) are balanced by costs in the elastic energy due to the deviations of s_i and $\Delta\theta_i = \theta_{i+1} - \theta_i$ from the equilibrium values ℓ_b and $\Delta\Theta$, respectively. For $s_i \neq \ell_b$ and/or $\Delta\theta_i \neq \Delta\Theta$, the pitch P is different from the equilibrium one $P_0 = (2\pi)/(\Delta\Theta)\ell_b$ and a twist energy is accumulated in the system. Moreover, the density of screw dislocations in the grain boundary changes following the Equation (1). Dislocation lines condensate and/or annihilate and, consequently, a condensation or annihilation energy is paid. In the following, we consider the distance between the smectic plane d and the angle δ between the director $\mathbf{n}$ and the normal to the smectic plane $\mathbf{N}$ in each block as constant (no electroclinical effect). This assumption is valid as long as the electric field amplitudes are not very large since d and δ are microscopic parameters. Experimental fields satisfy this condition. The total free energy per unit surface area in a transverse electric field is given by:

$$\begin{aligned} \mathcal{F}_T = \; & \sum_i \Big[\frac{B_1}{2}(s_i - \ell_b)^2 + \frac{B_2}{2}(\theta_{i+1} - \theta_i - \Delta\Theta)^2 + \\ + \; & B(\theta_{i+1} - \theta_i - \Delta\Theta)(s_{i+1} + s_i - 2\ell_b) - P_s E s_i \cos\theta_i\Big]. \end{aligned} \tag{3}$$

In $\mathcal{F}_T$ (3), we have considered only the lowest order terms in the deviation from the equilibrium values ℓ_b and $\Delta\Theta$. The first and second term in (3) represent the elastic energy cost to change the block thickness ($s_i \neq \ell_b$) and the angle between

blocks ($\Delta\theta_i \neq \Delta\Theta$), respectively. The third term in (3) couples the angle and the thickness deviations of the i^{th} block to the neighbours of rank $(i+1)^{th}$. In (3) we have omitted the anchoring energy since for the chosen configuration the electric field stabilizes the anchoring energy. Such a discrete model turns out to be very complex: for realistic experimental situations, the number of variables is of the order $25 \times 18 \times 2 = 900$. Let us discuss two limit cases.

1. $B_1 \gg B_2$

If $B_1 \gg B_2$, the TGB_C will relax the electric energy by keeping fixed the block thickness $s_i = \ell_b$ and by varying the angle between blocks. By putting in (3) $s_i = \ell_b$ for each block, we obtain a density energy $\mathcal{F}_{FK}$ given by:

$$\mathcal{F}_{FK} = \sum_i \left[\frac{B_2}{2} (\theta_{i+1} - \theta_i - \Delta\Theta)^2 - P_s E \ell_b \cos\theta_i \right]. \tag{4}$$

$\mathcal{F}_{FK}$ is analogous to the energy of a periodic chain of atoms in a periodic potential. It was originally introduced by Frenkel and Kontorova (FK) to explain the absorption of atoms on crystal substrates[13]. It also represents the energy of a series of coupled harmonic oscillators in a periodic potential. Solutions of the FK model were extensively studied by Aubry[14] as a function of the control parameter $\lambda = (P_s E \ell_b)/B_2$. Ground states for thermodynamical systems include periodic (i.e. commensurate) or quasi-periodic (i.e. incommensurate) solutions, but not chaotic state. We observed indeed that the contrast of the x-ray scattering modulation was strongly affected by the field. Such variations are consistent with periodic-quasi-periodic sequences. Note at last that unlike previously described systems, the TGB_C case allows an easy acces to the control parameter λ through the external field E.

2. $B_2 \gg B_1$

In this other limit, $B_2 \gg B_1$, the angle between blocks remains nearly fixed and the block thickness varies under the effect of the external field. In this limit $\mathcal{F}_T$ (3) has expression:

$$\mathcal{F}_T = \sum_i \left[\frac{B_1}{2} (s_i - \ell_b)^2 - P_s E s_i \cos(\Delta\Theta i) \right]. \tag{5}$$

The stationary solution which minimize $\mathcal{F}_T$ (5) is given by:

$$s_i = \ell_b + \alpha \cos(\Delta\Theta i), \tag{6}$$

where $\alpha = P_s E / B_1$. As predicted, the blocks with polarization nearly parallel to the electric field and, hence, with angles $-\pi/2 < \Delta\Theta i < \pi/2$, increase their size. The opposite is true, for polarization anti-parallel to the electric field ($\pi/2 <$

$\Delta\Theta i < 3\pi/2$). By increasing the field amplitude, the block size changes linearly with the electric field. A saturation term is needed in the energy (5) to prevent the block thickness to diverge in high field. The next higher order term we can add, is: $(D/4)(s_i - \ell_b)^4$. We can now minimize the new free density energy:

$$\mathcal{F}_T = \sum_i \left[\frac{B_1}{2}(s_i - \ell_b)^2 + \frac{D}{4}(s_i - \ell_b)^4 - P_s E s_i \cos(\Delta\Theta i) \right]. \quad (7)$$

To compare the model to the x-ray diffraction measurements, we simulate the χ-scan for the stationary configuration obtained. We calculate the intensity diffracted by the i^{th}-block as having a gaussian χ-profile centered at the block angle $\Delta\Theta i$, with amplitude proportional to the block thickness s_i and width 12° (FWHM). The total diffracted intensity is given by the superposition of the intensity profiles of each block.

In figures 2a-c are reported three simulated x-ray profiles of a TGB$_C$ with 18 blocks per pitch, for $\alpha/\ell_b = 0$, $\alpha/\ell_b = 0.3$ and $\alpha/\ell_b = 3$, respectively. In figures 2d-f are shown the experimental diffracted χ-scans for voltages $V = 0$, $V = 100V$ and $V = 250V$, respectively[15]. Under the field (figs. 2b-c and figs. 2e-f), parallel polarizations (defining $\chi = 0°$) are reinforced whereas antiparallel polarizations ($\chi = 180°$) are depressed.

For $V = 100V$ (fig. 2e), the number of peaks is increased but they become very irregular in shape and position. Their contrast is dramatically reduced. At the same time, a regular almost sinusoidal modulation of their amplitude shows up with a period of 360°. The maximum of this modulation sits along the direction $\chi = 0$ where the local polarizations are parallel to the external field. The sinusoidal modulation of the scattered intensity is qualitatively reproduced in the simulated scan (see fig.2(b)) whereas the contrast is about two times larger than in the experimental one. The reduction of the contrast can be explained by a small change in the angle between blocks so that the commensurability condition $(\theta_{i+1} - \theta_i) = \Delta\Theta = 2\pi/N$, with N integer, is no longer satisfied. The immediate effect is that the series of N equispaced peaks is disorganised: the χ-scan is now the projection of a distorted sequence of angles and is no longer regular.

At higher field ($V = 250V$), the amplitude of the modulation has increased. The envelope is rather square than sinusoidal, suggesting a strongly non linear behavior of the distortion. The trade off is clearly at 90°. Two distinct zones emerge: the range $-90° < \chi < 90°$ corresponds to a positive projection of local polarizations on the field and thus a negative electric energy (7) whereas the projections are negative in the other range $90° < \chi < 270°$. A series of peaks can be distinguished in the two regions, but still quite irregular. Their apparent periodicity, if any, is however not so much different from the zero field sequence. The region of negative projection exhibits no diffraction at all, which means that the corresponding slabs have disappeared, either because they have been rotated towards the "positive" region or because they have shrunk to zero thickness when grain boundaries have merged together. By changing the angle between two blocks from $\Delta\Theta$, at constant block thickness, we increase the twist energy of the TGB but we change also the

density of the network of dislocations in the grain boundaries. Thus, new dislocation lines must nucleates and/or annihilates and a large corresponding energy must be paid. In the opposite, if the blocks thickness varies at fixed angle, the cost in energy is essentially due to an increase of the twist energy. As a result the coefficient B_1 in (3) is expected much smaller than the corresponding B_2.

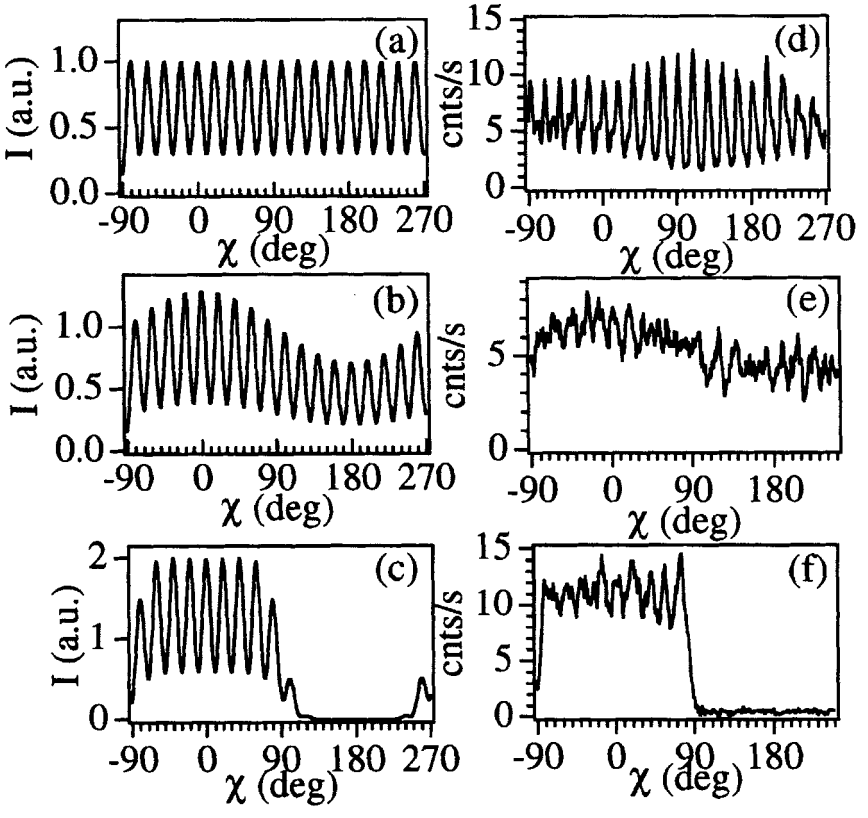

FIGURE 2 Simulated (a-c) and experimental (d-f) x-ray diffraction χ-scans of a TGB_C under transverse DC electric field.

Because the apparent periodicity of the remaining peaks is not very much changed, we think that the motion of grain boundaries is dominant. As a matter of fact, the simulated scan (fig.2f) reproduces quite good the experimental results.

In conclusion, in low electric field, the TGB_C relaxes the electric energy by increasing the size of block with polarization parallel to the electric field and by reducing, at the same time, the size of the antiparallel ones. The polarization of each block only weakly reorients along the electric field direction, by leaving, in this way almost unchanged the dislocations density in the grain boundaries.

REFERENCES

1. P.G. de Gennes, Solid State Commun. 10, 753 (1972).
2. A.A. Abrikosov, Zh. Eksp. Teor. fiz. 32, 1442 (1957) [Sov. Phys. JETP 5, 1174 (1957)].
3. J.W. Goodby, M.A. Waugh, S.M. Stein, E. Chin, R. Pindak and J.S. Patel, Nature (London) 337, 449 (1989); J. Am. Chem. Soc. 111, 8119 (1989).
4. S.R. Renn and T.C. Lubensky, Phys. Rev. A 38, 2132 (1988).
5. H.T. Nguyen, A. Bouchta, L. Navailles, P. Barois, N. Isaert, R.J. Twieg, A. Maaroufi and C. Destrade, J. Phys. II (France) 2, 1889 (1992).
6. L. Navailles, P. Barois and H.T. Nguyen, Phys. Rev. Lett. 71, 545 (1993).
7. L. Navailles, H.T. Nguyen, P. Barois and N. Isaert, Mol. Cryst. Liq. Cryst. (1996)
8. Y. Galerne, Phys. Rev. Lett. 72, 1299 (1994) L. Navailles, P. Barois and H.T. Nguyen, Phys. Rev. Lett. 72, 1300 (1994).
9. R.B. Meyer, L. Liébert, L. Strzelecki and P. Keller, J. Phys. Lett. 36, 69 (1975).
10. S.R. Renn and T.C. Lubensky, Mol. Cryst. Liq. Cryst. 209, 349 (1991).
11. S. Renn, Phys. Rev. A 45, 953 (1992).
12. L. Navailles, R. Pindak, P. Barois and H.T. Nguyen, Phys. Rev. Lett. 74 (1995).
13. T. Kontorova and Y.I. Frenkel, Zh. Eksp. and Teor. Fiz. 8, 89, 1340 (1938)
14. S. Aubry and P.Y. Le Daeron, Physica 8D 381 (1983)
15. M.Petit, P. Barois and H.T. Nguyen, submitted to Europhysics Lett.